Journal of Statistical Physics, Vol. 106, Nos. 3/4, February 2002 (© 2002)

Modeling of the Dielectric Breakdown Under Strong Magnetic Fields

Y. Ben-Ezra,[1, 2, 3] **Yu. V. Pershin,**[1, 4, 5] **Yu. A. Kaplunovsky,**[1, 2] **I. D. Vagner,**[1, 5] **and P. Wyder**[1, 6]

Received May 8, 2001; accepted July 25, 2001

The formation of breakdown pattern on an insulating surface under the influence of a transverse magnetic field is theoretically investigated. We have generalized the Dielectric Breakdown Model (DBM) and random walker model for the case of external magnetic field. It is shown that fractal dimensionality of the discharge saturates with magnetic fields. It is conjectured that nonlinear current interaction is responsible for the experimentally observed "spider-legs" like streamer patterns.

KEY WORDS: Surface discharge; streamer; fractal; fractal dimensionality

Fractal properties are common to the dielectric breakdown phenomena[1] which range from an atmospheric lightning[2–4] to electric treeing in polymers[5] and are of significant scientific and technical importance.[6, 7] Although the actual physical processes could be quite different in these phenomena, the global properties of the resulting discharge patterns are very similar. Filamentary gas discharges on insulating surface exhibit remarkable similarities to breakdown phenomena in long gaps,[8] e.g., to atmospheric lightning, and thus offer the possibility to perform well-defined model experiments in laboratory.

[1] Grenoble High Magnetic Fields Laboratory, Max-Planck-Institute für Festkorperforschung and CNRS, 25 Avenue des Martyrs, F-38042, Grenoble, France.
[2] P.E.R.I.-Physics and Engineering Research Institute at Ruppin, Emek Hefer 40250, Israel.
[3] School of Physics and Astronomy, Tel Aviv University, Tel Aviv 69978, Israel.
[4] B. I. Verkin Institute for Low Temperature Physics and Engineering, 47 Lenin Avenue, 310164 Kharkov, Ukraine.
[5] Holon Academic Institute of Technology, 52 Golomb St., Holon 58102, Israel.
[6] Corresponding author: MPI-CNRS, 25 Avenue des Martyrs, BP 166, F-38042, Grenoble, France; e-mail: wyder@polycnrs-gre.fr

0022-4715/02/0200-0653/0 © 2002 Plenum Publishing Corporation

The surface discharge in compressed SF_6 gas has been studied in detail by Niemeyer and Pinnekamp.[9] The parameters were controlled in such a way that the experiment produces, to a good approximation, an equipotential channel system growing in a plane with a radial electrode from a central point. The experiment shows that the dielectric breakdown pattern has a fractal structure. The stochastic model containing the essential features of the fractal properties of the dielectric breakdown was introduced by Niemeyer, Pietroniero, and Wiesmann (NPW),[1, 10] and generalized by Wiesmann and Zeller.[11]

In the recent experiment[3] a transverse high magnetic field was applied during the discharge evolution and thus any spatial restriction of the surface discharge was avoided in order to use a locally sensitive probe. The experiment shows the spatial evolution of a negative surface discharge in a nitrogen atmosphere as a function of the magnetic field (Fig. 1). At $B = 0$ a very bright starlike pattern develops (Fig. 1a). At moderate magnetic field (up to $7T$), the leader channels are bent and appear to have a circular shape outside the central electrode region (Fig. 1b).

The radius of curvature is of the order of 1 cm at $7T$. The direction of the bending corresponds to the movement of electrons in crossed electric and magnetic fields. With the increase of the magnetic field the radius of curvature decreases, the channels approach each other and branching sets in. At the highest applied magnetic field of $12T$ (Fig. 1c), the circular-shaped current filaments are only found in the outmost regions of the discharge pattern where they can develop undisturbed by the fields of neighboring leader channels.

In this letter we modify the DBM model introduced by Wiesmann and Zeller[11] and the active walker model[12, 13] for the case of external magnetic field.

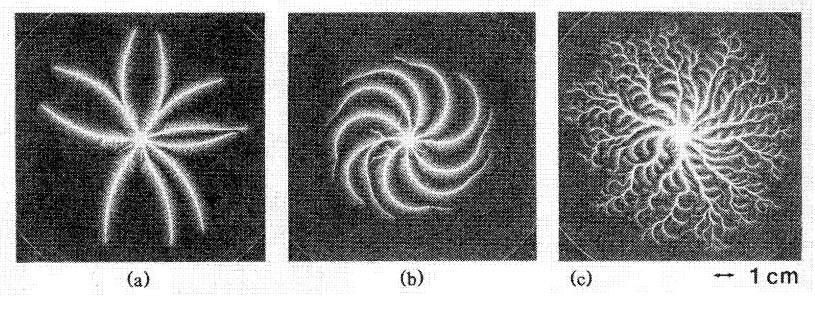

Fig. 1. Surface discharge patterns in N_2 at atmospheric pressure for different external magnetic fields (Fig. 2 from ref. 3): (a) $B = 0T$; (b) $B = 5T$; (c) $B = 12T$.

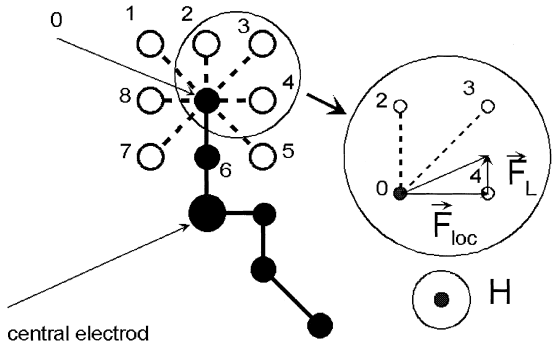

Fig. 2. Bonds connecting a lattice point with one of eight adjacent lattice points in a two-dimensional square lattice. The geometry of the experiment is represented by a central electrode at some point while the other electrode is a circle at large distance. The discharge starts at the central electrode and grows by one lattice bond per growth step.

Let us consider a two-dimensional square lattice in which a central point represents one of the electrodes while the other electrode is modeled as a circle at large distance (Fig. 2), according to the geometry of the experiment.[3] The discharge starts at the central electrode and grows by one lattice bond per growth step. A bond connects a lattice point with one of eight adjacent lattice points as it is described in Fig. 2. Once a given point is connected to the discharge structure by a bond, it becomes part of the structure. The potential of the central electrode is 0, the potential of a point in the structure is $V_{i,k} = V_{l,m} + V_R * l$, where $V_{l,m}$ is the potential of a points from which growth go on, V_R is an internal field in the structure and l is 1 for bonds parallel to the grid and is $\sqrt{2}$ for diagonal bonds.

The growth is computed as follows: first the Laplace equation is solved with the boundary conditions determined by the electrodes and the discharge structure. Then the local field F_{loc} between a point which is already a part of the structure (i, k) and a new adjacent point (i', k') is $F_{\text{loc}}(i, k, i', k') = \frac{\varphi_{i',k'} - V_{i,k}}{l}$, where $\varphi_{i',k'}$ is the solution of Laplace equation. The breakdown can occur only if the local field is greater than the critical field of growth F_C. The probability that a new bond will form between a point which is already a part of the structure and a new adjacent point $p(i, k \to i', k')$ is calculated as a function of the local field F_{loc} between the two points:

$$p(i, k \to i', k') = \frac{F_{\text{loc}}^{\eta}}{\sum F_{\text{loc}}^{\eta}} \tag{1}$$

where a power-low dependence with exponent η is assumed to describe adequately the relation between the local field and the probability. The sum in the denominator refers to all possible growth processes. A new bond is chosen randomly with probability distribution (1) and added to the discharge pattern. With this new discharge pattern one starts again. More detailed description of this model is done in ref. 11.

Application of an external magnetic field changes the probability distribution (1). A moving charge in the magnetic field experiences the Lorentz force $\vec{F_L} = e\vec{V} \times \vec{H}$, which is perpendicular to $\vec{V}$, the charge velocity. Here e is the electron charge and $\vec{H}$ is the magnetic field. Consider each step of growth like a superposition of two processes. The first step is choosing a new bond using the probability distribution (1), and the second step is taking into account the probability, p_H, of deviation of the growth due to the magnetic field.

Suppose, for example, that after first step of growth the bond from the dot 0 to the dot 4 was chosen (Fig. 2). In the next step, then, the growth will proceed from the dot 0 to the dot 3 with the probability p_H or to the dot 4 with the probability $1-p_H$. The new probability of growth can be written as

$$\tilde{p}(i, k \to i', k') = \frac{p(i, k \to i', k')(1-p_H(i, k, i', k')) + p(i, k \to i'', k'')\, p_H(i, k, i'', k'')}{\sum (p(i, k \to i', k')(1-p_H(i, k, i', k')) + p(i, k \to i'', k'')\, p_H(i, k, i'', k''))} \tag{2}$$

where the point (i'', k'') is the neighboring point with respect to the point (i', k') in the clockwise direction with respect to the point (i, k) and the sum in the denominator refers to all possible growth processes. The probability (2) was used in computer simulations in place of the probability (1) with the same algorithm.

Let us turn to the probability p_H of deviation of the growth due to the magnetic field. In our model, during the process of growth, two constant forces act on charge carriers, F_L and eF_{loc} (Fig. 2). When the resulting force is near the dot 3, $p_H \to 1$; when the resulting force is near the dot 4, $p_H \to 0$. It is clear that the probability p_H is proportional to $\frac{F_L}{eF_{\text{loc}}}$. If $eF_{\text{loc}}(i, k, i', k') < F_C$ then the growth does not occur and p_H should be zero. If $\frac{F_L}{eF_{\text{loc}}} > 1$ then we let $p_H = 1$. The force F_L is proportional to the velocity of charge carrier. In our model we can take into account only a local velocity, which arrises in the first step of growth process due to the acceleration of the charges in the local field F_{loc} on a some characteristic

length δl. The velocity of charge carriers can be estimated from the energy conservation law. So, the value of the effective Lorentz force is:

$$F_L(i,k,i',k') = e\sqrt{\frac{2e}{m}\,\delta l F_{\text{loc}}(i,k,i',k')}\;H \tag{3}$$

where m is an effective mass. Based on these considerations, we choose the probability of deviation of the growth due to the magnetic field, p_H, in the following form:

$$p_H(i,k,i',k') = \begin{cases} 0, F_{\text{loc}}(i,k,i',k') < F_C \\ \dfrac{F_L(i,k,i',k')}{F_{\text{loc}}(i,k,i',k')}, \dfrac{F_L(i,k,i',k')}{F_{\text{loc}}(i,k,i',k')} \leqslant 1, F_{\text{loc}}(i,k,i',k') \geqslant F_C \\ 1, \dfrac{F_L(i,k,i',k')}{F_{\text{loc}}(i,k,i',k')} > 1, F_{\text{loc}}(i,k,i',k') \geqslant F_C \end{cases} \tag{4}$$

where $F_L(i,k,i',k') = \sqrt{lF_{\text{loc}}(i,k,i',k')}\;H$ and H is the value of the magnetic field.

In our computer simulations we consider a 500×500 lattice. The solutions of the Laplace equation were obtained by the iteration method.[10] Before starting of each realization of growth we performed 20000 iterations and after each step of growth the number of iterations was 40. This procedure gives a good convergence. The number of particles in breakdown structure was 9000.

The fractal dimension was calculated by the method described in ref. 10, where for every realization the $\log N(R)$ versus $\log R$ is plotted. Here $N(R)$ is the number of particles belonging to the structure and being within a circle of radius R. The fractal dimension is obtained by fitting a straight line to the data scaling region. For every set of the same parameters of the model (H, F_C, V_R, η) we made about 100 realizations. Thus the statistical fluctuations were reduced.

We start our simulations with the case of the zero magnetic field and the zero values of the parameters Fc and V_R in order to compare our results with the results of the different authors. Our results for this set of parameters are in a good agreement with the results, obtained in refs. 10 and 11.

The example of the computer-generated discharge pattern (Lichtenberg figure[2]) corresponding to the following set of parameters: $H = 0$, $\eta = 1$, $F_c = 0$ and $V_R = 0$ is shown in Fig. 3a. In Fig. 3b we show the computer-generated discharge pattern in the presence of the external magnetic field. The white lines in Figs. 3a and 3b correspond to the leader channels.

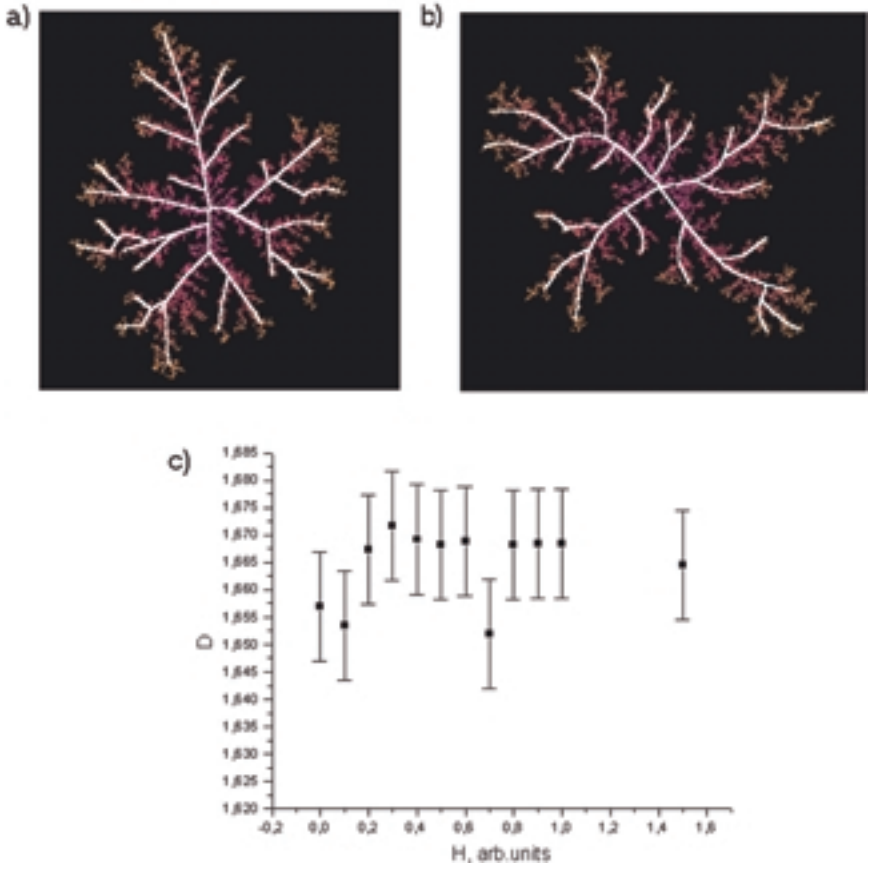

Fig. 3. (a) Computer-generated discharge pattern (Lichtenberg figure) corresponding to the following set of parameters: $H = 0$, $\eta = 1$, $F_c = 0$ and $V_R = 0$ as explained in the text. The white lines correspond to the leader channels; (b) computer-generated discharge pattern in the presence of the external magnetic field. The leader channels in the magnetic field are distorted and appear to have a circular shape outside the central electrode region, due to the action of the magnetic field; (c) the saturation of the fractal dimensionality, with growing magnetic fields, at the value of $D = 1.67$.

Unlike the pattern, presented in Fig. 3a, the leader channels in the magnetic field are distorted and appear to have a circular shape outside the central electrode region. The direction of the bending corresponds to the movement of electrons in crossed electric and magnetic field. The radius of curvature of the leader channel is about two orders of magnitude greater then the Larmor radius of an electron.

The saturation of the fractal dimensionality, with growing magnetic fields, at the value of $D = 1.67$, is presented in Fig. 3c. The plot starts from the value of $D = 1.65$, in the absence of magnetic field, which is smaller than the fractal dimensionality reported in ref. 10. Such difference results from the fact that in ref. 10 the critical field value for the breakdown was not taken into account. We have improved their calculations by introducing the minimal value of the electric field for the breakdown between two successive points. In this case the breakdown pattern is more directionally selected, and a lower fractal dimensionality results. With the increase of the external magnetic field, the fractal dimension growth and finally saturates at an universal for high magnetic fields values of 1.67 ± 0.01. We introduce here a preliminary notion of Magnetic Fractal Dimensionality (MFD). The growth of MFD with the magnetic field could be expected, since the curved trajectories fill up the space more densely than the straight ones. The existence of an universal limit, however, is far from being obvious. Following the directed percolation models, one could think that the saturation of MFD will occur at $D = 2$. Figure 3c shows clearly that in this system the MFD saturates due to the physics of current carrying streamers.

An unexplained feature of the experiments[3] is the "spider-legs" form of the breakdown pattern in the absence of the external magnetic field. We outline here that the streamer currents are rather strong, $10 \div 100A$, and their influence on the streamer pattern can be very important. To describe this phenomenon we have taken into account the magnetic interaction between current carrying streamers, in the framework of the modified active walker model which is described in what follows. The results of our calculations, presented in Fig. 4, show that our model correctly describes the experimentally observed "spider-legs" effect.

Active walker models have been used to describe different pattern formation problems.[12, 13] In these models the walkers movement is subject to the influences of the environment and vice versa. We describe the leader channel propagation in the magnetic field using the active walker model. The Lorentz force acting on the fast-moving electrons is particularly effective in the high-field regions in the leader tips, where the channel formation takes place.

Let us consider again a two-dimensional square lattice in which a central point represents one of the electrodes while the other electrode is modeled as a circle at large distance. The discharge starts at the central electrode, so initially several walkers are set in the vicinity of it. The walkers move in a potential which is the solution of the Laplace equation with the boundary conditions determined by electrodes and discharge structure. During a step of growth each walker moves. The solution of Laplace equation is found by iteration method[10] after each step of growth.

When a walker moves to a point, this point starts belonging to the breakdown structure. The potential of the central electrode is 0, the potential of the points in the structure is $V_{i,k} = V_{l,m} + V_R * l$, where $V_{l,m}$ is the potential of a points from which growth go on, V_R is an internal field in the structure and l is 1 for bonds parallel to the grid and is $\sqrt{2}$ for diagonal bonds. In the absence of the magnetic field, the probability of a walker step is a function of the local field F_{loc}.[12] The breakdown occurs only if the local field is greater then the critical field of growth F_C.

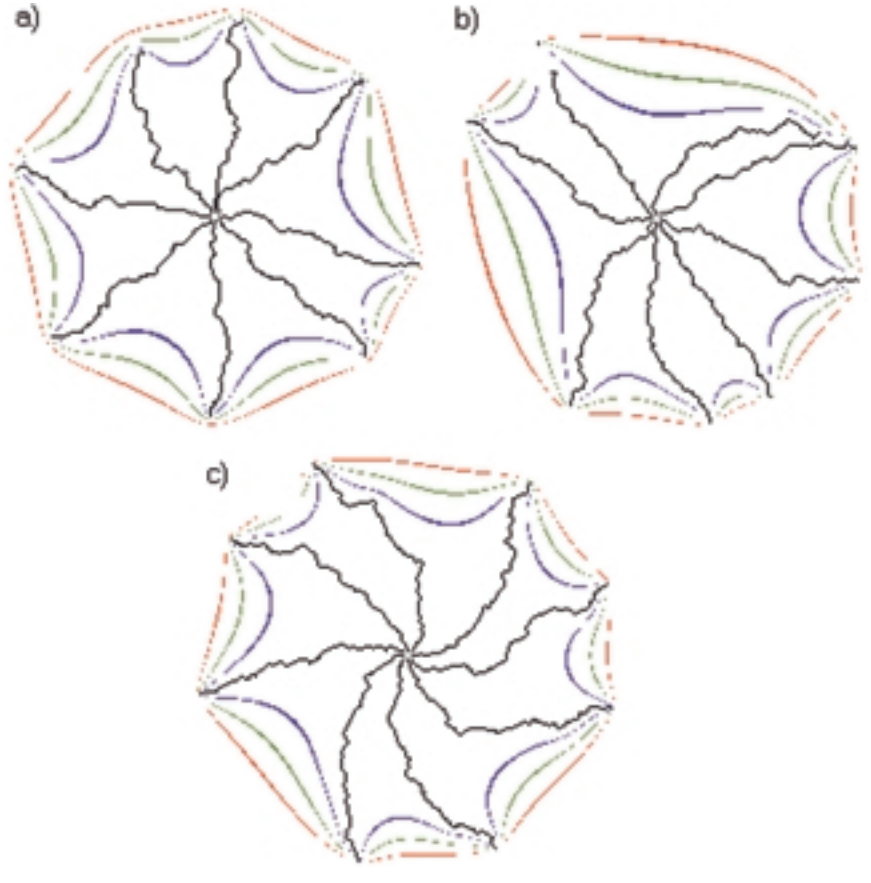

Fig. 4. The "spider-legs" form of the breakdown pattern following from the magnetic interaction between the streamer currents: (a) current-current interactions are not taken into account, $H = 0$; (b) current-current interactions are included into calculations, $H = 0$; (c) current-current interactions are included into calculations, $H \neq 0$. The color lines are equipotential surfaces.

The magnetic field is taken into account by the following way. We add to the local field in the direction perpendicular to the previous move of the walker the Lorentz force which is proportional to the magnetic field. The magnetic field acting on the i walker is $H_i = H_0 + H_I^i$, where H_0 is external magnetic field and H_I^i is the field created by currents of the breakdown structure. We calculate H_I^i by means of the Biot–Savart law.

The main results of this part of studies are presented in Fig. 4.

To summarize, the main results of this paper are as follows.

(1) Our model based on generalized DBM describes well the growing of the discharge pattern complexity in the magnetic field. As in experiments, the radius of the curvature decreases with increasing of the magnetic field. This radius is much larger than the electron cyclotron orbit and results from the drift movement of the Larmor centers of the qyrating electrons.[3]

(2) We have introduced a preliminary concept of the Magnetic Fractal Dimensionality and have obtained its saturation with growing magnetic fields. The Universal Magnetic Fractal Dimensionality equals 1.670 which is superior to 1.65, obtained in the absence of a magnetic field.

(3) The results obtained with the use of modified active walker model are in a good agreement with experiment. The magnetic interaction between the current-carrying streamers results in the "spider-legs" like streamer patterns at lower fields, which corresponds to the experimental observations.

ACKNOWLEDGMENTS

We acknowledge helpful discussions with T. Maniv and A. Zhuravlev. I.V. and Yu.K. acknowledge the support by the Caesarea Edmond Benjamin de Rothschild Foundation.

REFERENCES

1. A. Erzan, L. Pietronero, and A. Vespignani, *Reviews of Modern Physics* **67**, No. 3 (1995).
2. G. C. Lichtenberg, *Novi Commentarii Societatis Regiae Scientiarium Gottingae* **8**:168 (1877).
3. P. Uhlig, J. C. Maan, and P. Wyder, *Phys. Rev. Lett.* **63**:1968 (1989).
4. *Engineering Dielectrics*, Vols I–VI (American Society for Testing and Materails, Philadelphia, 1983), Special Technical Publication No. LC. No82-70637.
5. R. A. Fava, in *Treatise on Material Science and Technology*, J. M. Schutz, ed. (Academic, New York, 1977), Vol. 10, Pt. B., p. 677.
6. H. R. Zeller and W. R. Schneider, *J. Appl. Phys.* **56**:455 (1984).
7. Tamas Vicsek, *Fractal Growth Phenomena* (World Scientific Publishing, 1989).
8. I. Gallimberti, *J. Phys. (Paris), Colloq.* **40**:C7–197 (1979).

9. L. Niemeyer and F. Pinnekamp, in *Gaseous Dielectrics III*, G. Christophorou, ed. (Pergamon, New York, 1982).
10. L. Niemeyer, L. Pietronero, and H. J. Wiesmann, *Phys. Rev. Lett.* **52**:1033 (1984).
11. H. J. Wiesmann and H. R. Zeller, *J. Appl. Phys.* **60**(5):1770 (1986).
12. Chia-Rong Sheu, Ching-Yen Cheng, and Ru-Pin Pan, *Phys. Rev. E* **59**:1540 (1999).
13. D. Helbing, F. Schweitzer, J. Keltsch and P. Molnar, *Phys. Rev. E* **56**:2527 (1997).